

---

# CaliDrop: KV Cache Compression with Calibration

---

**Yi Su<sup>1</sup>, Quantong Qiu<sup>1</sup>, Yuechi Zhou<sup>1\*</sup>, Juntao Li<sup>1\*</sup>**  
**Qingrong Xia<sup>2</sup>, Ping Li<sup>2</sup>, Xinyu Duan<sup>2</sup>, Zhefeng Wang<sup>2</sup>, Min Zhang<sup>1</sup>**  
<sup>1</sup>School of Computer Science and Technology, Soochow University  
<sup>2</sup>Huawei Cloud  
yisunlp@outlook.com; {ljt, minzhang}@suda.edu.cn

## Abstract

Large Language Models (LLMs) require substantial computational resources during generation. While the Key-Value (KV) cache significantly accelerates this process by storing attention intermediates, its memory footprint grows linearly with sequence length, batch size, and model size, creating a bottleneck in long-context scenarios. Various KV cache compression techniques, including token eviction, quantization, and low-rank projection, have been proposed to mitigate this bottleneck, often complementing each other. This paper focuses on enhancing token eviction strategies. Token eviction leverages the observation that the attention patterns are often sparse, allowing for the removal of less critical KV entries to save memory. However, this reduction usually comes at the cost of notable accuracy degradation, particularly under high compression ratios. To address this issue, we propose **CaliDrop**, a novel strategy that enhances token eviction through calibration. Our preliminary experiments show that queries at nearby positions exhibit high similarity. Building on this observation, CaliDrop performs speculative calibration on the discarded tokens to mitigate the accuracy loss caused by token eviction. Extensive experiments demonstrate that CaliDrop significantly improves the accuracy of existing token eviction methods.

## 1 Introduction

Large language models (LLMs) have demonstrated remarkable capabilities across various domains [1, 31, 10, 17, 22]. However, their auto-regressive generation process often results in slow inference speeds. KV cache reduces the computational complexity of self-attention from  $O(n_2)$  to  $O(n)$  by storing intermediate key-value pairs from previous attention operations. This allows the model to avoid recalculating these values in future attention computations, thus speeding up inference. However, this efficiency comes at the cost of additional memory usage, as the KV cache must store the key-value pairs for each token. The memory overhead of the KV cache grows linearly with the sequence length, which becomes particularly severe in long-context scenarios [35], posing substantial deployment challenges and creating the need for effective KV cache compression solutions.

Existing KV cache compression methods include quantization [19, 25], layer-wise sharing [34, 4], prefix sharing [18, 45], head-wise sharing [27, 2], token eviction [20, 43], and low-rank projection [32, 39]. Our work focuses on token eviction, which reduces memory consumption by removing non-critical tokens from the KV cache. Current token eviction methods typically leverage the observation that a small subset of tokens contributes to the majority of attention scores. For example, StreamingLLM [35] argues that the tokens at the beginning and those closest to the current token have higher attention scores. H2O [43] estimates the importance of each token by using the accumulated attention score. SnapKV [20] estimates token importance using an observing window and the pooled

---

\* Corresponding author.

accumulated attention score. However, these approaches face two fundamental limitations in high compression ratio scenarios: (1) Permanently discarding tokens can be detrimental to accuracy if those tokens later become crucial, and (2) the coarse-grained removal process often leads to significant accuracy degradation [38].

To address these limitations, we propose CaliDrop, a novel strategy that enhances token eviction methods through calibration. Our key insights are based on two empirical observations: (1) Queries at nearby positions exhibit high similarity, and (2) Historical attention outputs can be used to predict future attention outputs. Building on these insights, CaliDrop compensates for evicted tokens by precomputing attention outputs for queries at nearby positions, alleviating memory pressure while maintaining model accuracy. Extensive experiments demonstrate that CaliDrop significantly enhances the accuracy of existing token eviction methods.

In summary, our contributions are as follows:

- We analyze the similarity between queries of the model and find that queries at nearby positions typically exhibit higher cosine similarity.
- We propose CaliDrop, a general strategy that can be integrated with existing token eviction methods to effectively approximate compensation for evicted tokens, thus improving accuracy under high compression ratios.
- Experiments on different benchmarks, models, and compression ratios have demonstrated that our method significantly improves accuracy over existing token eviction methods.

## 2 Related work

**KV Cache Compression.** KV cache compression is essential for reducing memory usage and improving efficiency in Large Language Models, allowing faster inference and deployment on resource-constrained scenarios. There are different methods for KV cache compression. Low-rank approximation [19, 6] compresses KV cache by leveraging their low-rank structure. Group Query Attention (GQA) [2] and Multi-Query Attention (MQA) [27] share KV cache within different heads to reduce redundancy. Multi-Head Latent Attention (MLA) [21] down-projects KV cache to low-rank spaces for memory optimization. Token eviction [43, 35, 20] discard some unimportant tokens during generation, in order to reduce the size of the KV cache while preserving higher accuracy as much as possible. KV cache quantization [28, 25, 15, 14, 40, 9, 38] stores unimportant tokens in lower precision and retains important ones in full precision. Inter-layer KV sharing [29, 34, 4] reduces memory usage by allowing different layers to share the same KV cache, significantly lowering redundancy across layers. Prefix sharing [18, 45] shares common prefixes among different sequences to reduce redundancy. KV merging [33, 42] uses reparameterization and interpolation techniques to reduce redundancy while preserving semantic integrity. These approaches are often orthogonal and can typically be combined to achieve superior compression results and efficiency gains.

**Token Eviction.** To reduce memory usage, eviction-based strategies keep a fixed KV cache size to store critical KV pairs and discard unnecessary pairs. Most methods evaluate token importance based on attention scores. As demonstrated in [24, 43, 20], tokens with higher accumulated attention scores are considered more important. Alternative strategies employ factors such as initial tokens [35], special tokens [13, 7], or L2 norms [8]. Recent studies focus on optimizing the allocation of the KV cache memory budget. Some focus on cross-layer strategies, where PyramidKV [5] and PyramidInfer [37] utilize a pyramid-shaped memory allocation while selecting tokens with high attention scores in each layer. CakeKV [26] dynamically analyzes the attention patterns of each layer during the prefill stage to adaptively allocate KV cache sizes. DynamicKV [44] computes the average attention scores of recent and historical tokens, allocating budgets proportionally based on the density of critical tokens in each layer. Other works focus on head-level allocation strategies. AdaKV [11] optimizes L1 loss between original and pruned multi-head attention outputs for head-wise budget assignment. LeanKV [41] optimizes KV cache management through heterogeneous quantization, dynamic sparsity, and unified compression. HeadKV [12] evaluates the retrieval and reasoning performance to optimize the KV cache allocation. In order to minimize redundancy and mitigate information loss due to the token eviction strategy, researchers have proposed several innovative methods. For example, Cam [42] and KVMerger [33] merge less important tokens into a single token based on similarity in attention patterns. Additionally, RecycledAttention [36] recalculates previously deemed unimportant tokens at regular intervals to select the top-k important tokens.

### 3 Method

#### 3.1 Preliminary Experiments

While prior studies indicate historical attention scores can approximate future patterns [43, 20], the predictive power of historical queries and the utility of historical attention outputs for future approximations remain less explored. To establish a foundation for our proposed method, we conduct preliminary experiments addressing two key questions: (1) Can historical queries approximate future queries? (2) Can historical attention outputs help approximate future attention outputs?

##### 3.1.1 Q1: Can Historical Queries Approximate Future Queries?

To investigate whether historical queries can approximate future queries, we conduct experiments using LLaMA-3-8b-Instruct [10] on LongBench [3]. We retain all queries of Layer 10, Head 16 during inference and calculate the cosine similarity between each of them. Figure 1 (top-right) presents a heatmap of the cosine similarity of queries in a single sample (we plot the results of token positions from 50-150 for simplicity). While we show only one figure for clarity, similar trends are observed across other layers, heads, tokens and samples. The heatmap indicates that queries at nearby positions exhibit high cosine similarity, suggesting that historical queries indeed provide a reliable approximation for future queries.

##### 3.1.2 Attention Decomposition Theorem

Before answering Q2, we propose a theoretical foundation for splitting attention computation. Let  $Q$  be the Query of the current tokens, and let  $K, V$  represent the Key and Value of a set of  $n$  tokens  $S = \{t_1, \dots, t_n\}$  in the KV cache. Consider a partition of the tokens into disjoint subsets  $S_i$  and  $S_j$  such that  $S_i \cup S_j = S$ . Let  $K_{S_i}, V_{S_i}$  and  $K_{S_j}, V_{S_j}$  be the corresponding subset of  $K$  and  $V$ . The attention computation over the full set  $S$  can be decomposed as follows:

$$\text{Att}(Q, K, V) = \alpha_i \cdot \text{Att}(Q, K_{S_i}, V_{S_i}) + \alpha_j \cdot \text{Att}(Q, K_{S_j}, V_{S_j}) \quad (1)$$

Where the weights  $\alpha_i$  and  $\alpha_j$  represent the normalized exponential sum of the attention weights from each subset:

$$\alpha_i = \frac{\sum_{t \in S_i} e^{\frac{QK_t^\top}{\sqrt{d_k}}}}{\sum_{t \in S} e^{\frac{QK_t^\top}{\sqrt{d_k}}}}, \quad \alpha_j = \frac{\sum_{t \in S_j} e^{\frac{QK_t^\top}{\sqrt{d_k}}}}{\sum_{t \in S} e^{\frac{QK_t^\top}{\sqrt{d_k}}}} \quad (2)$$

Note that  $\alpha_i + \alpha_j = 1$ . This decomposition allows for the independent attention computation of the subsets and is crucial for our hybrid attention computation strategy.

*Proof.*

$$\begin{aligned} \text{Att}(Q, K, V) &= \text{softmax} \left( \frac{QK^\top}{\sqrt{d_k}} \right) V = \frac{\sum_{t \in S} e^{\frac{QK_t^\top}{\sqrt{d_k}}} V_t}{\sum_{t \in S} e^{\frac{QK_t^\top}{\sqrt{d_k}}}} \\ &= \frac{\sum_{t \in S_i} e^{\frac{QK_t^\top}{\sqrt{d_k}}} V_t + \sum_{t \in S_j} e^{\frac{QK_t^\top}{\sqrt{d_k}}} V_t}{\sum_{t \in S} e^{\frac{QK_t^\top}{\sqrt{d_k}}}} \\ &= \frac{\sum_{t \in S_i} e^{\frac{QK_t^\top}{\sqrt{d_k}}}}{\sum_{t \in S} e^{\frac{QK_t^\top}{\sqrt{d_k}}}} \cdot \frac{\sum_{t \in S_i} e^{\frac{QK_t^\top}{\sqrt{d_k}}} V_t}{\sum_{t \in S_i} e^{\frac{QK_t^\top}{\sqrt{d_k}}}} + \frac{\sum_{t \in S_j} e^{\frac{QK_t^\top}{\sqrt{d_k}}}}{\sum_{t \in S} e^{\frac{QK_t^\top}{\sqrt{d_k}}}} \cdot \frac{\sum_{t \in S_j} e^{\frac{QK_t^\top}{\sqrt{d_k}}} V_t}{\sum_{t \in S_j} e^{\frac{QK_t^\top}{\sqrt{d_k}}}} \\ &= \alpha_i \cdot \text{Att}(Q, K_{S_i}, V_{S_i}) + \alpha_j \cdot \text{Att}(Q, K_{S_j}, V_{S_j}) \end{aligned} \quad (3)$$

##### 3.1.3 Q2: Can Historical Attention Outputs Help Approximate Future Attention Outputs?

In this part, we investigate whether historical attention outputs can be used to approximate future attention outputs. Directly multiplying the historical query with the KV cache is not feasible, as

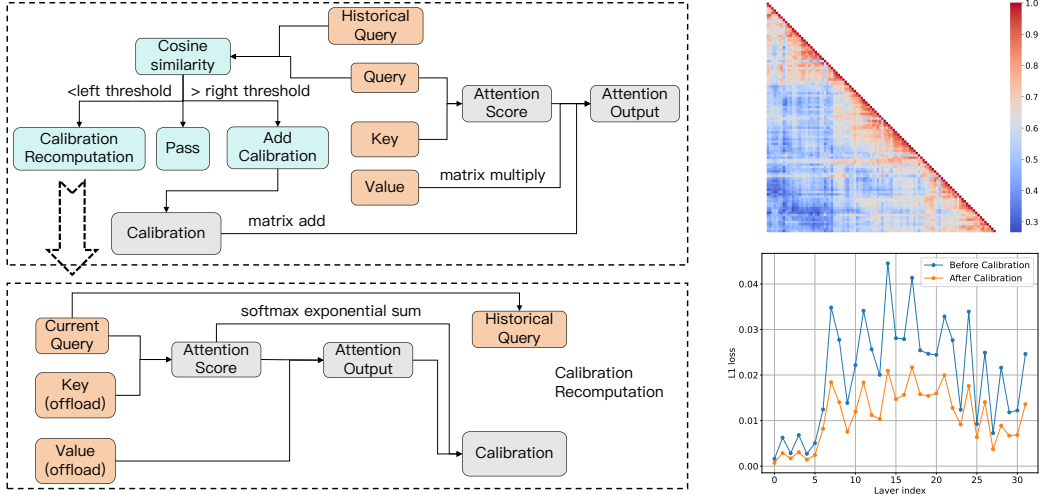


Figure 1: Illustration of the proposed method and preliminary results. Left: Overview of the method in decoding. We first compute the cosine similarity between the current query and historical query, and then decide whether to perform recomputation, apply calibration, or take no action based on the similarity. Top-right: the heatmap of cosine similarity of the queries in an example. Bottom-right: L1 loss before and after calibration.

it would discard the information from the current query entirely. Therefore, we propose a method that splits the KV cache into two parts (important & unimportant) inspired by the token eviction methods. We compute the current query with the important KV cache and the historical query with the unimportant KV cache. We integrate the two results according to Equation 1 as the final attention output to approximate the true current attention output. We refer to this integration process as **calibration**, which is the core of our method.

To preliminarily validate the effectiveness of this method, we conduct experiments using LLaMA-3-8b-Instruct [10] on LongBench [3]. We use the token eviction strategy from SnapKV [20] to select 128 important tokens and other tokens are considered unimportant. We set the current token to be the first token after the prefill phase. We set the historical token to be one of the 0-9th tokens preceding the current token (randomly selected). We compare the L1 loss of the approximated attention output and the true current attention output before and after calibration across different layers.

Theoretically, if the historical query is completely the same as the current query, the L1 loss should be 0. When the historical and current queries are highly similar, we expect the calibration to provide a positive effect. Conversely, if the queries are not similar, there will be a side effect. Figure 1 (bottom-right) shows the L1 loss before and after calibration across different layers. The results demonstrate that adding calibration significantly reduces the L1 loss. Similar trends are observed across other tokens and samples, although additional figures are omitted for brevity. From these findings, we conclude that historical attention outputs can help approximate future attention outputs.

### 3.2 CaliDrop

After the aforementioned preliminary results, we introduce **CaliDrop**. CaliDrop can be applied on top of existing token eviction methods to enhance accuracy. Following SnapKV [20], we focus on token eviction during prefilling, although our method can be easily extended to the decoding phase.

After token eviction based on a certain strategy, we do not directly delete the evicted KV cache. Instead, we offload them. At this point, we use the current query to perform attention computation with the evicted KV cache. After computation, we retain the current query, the softmax denominator, and the attention output for future calibration during subsequent attention computations. In the decoding phase, we add calibration according to Equation 1. However, the similarity between the current query and the historical query decreases as the positional difference increases. Thus, we need to ensure that the added calibration mostly provides a positive effect. To address this, we introduce two hyper-parameters: the left threshold ( $\theta_1$ ) and the right threshold ( $\theta_2$ ). These thresholds control

---

**Algorithm 1** CaliDrop Prefill

---

**Require:** Input sequence  $X$ , eviction strategy  $f$

- 1: Compute all queries  $Q$ , keys  $K$ , values  $V$  for input  $X$
- 2: Compute attention outputs for current query: Output =  $\text{Att}(Q, K, V)$
- 3: Select important tokens using eviction strategy:  $KV_{\text{compress}} \leftarrow f(Q, K, V)$
- 4: Offload evicted KV pairs:  $KV_{\text{evict}} \leftarrow KV_{\text{full}} \setminus KV_{\text{compress}}$
- 5: Compute calibration using the last query:
- 6:  $C_{\text{weight}} = \sum \exp\left(\frac{Q_{-1} * K_{\text{evict}}^T}{d_k}\right)$
- 7:  $C_{\text{out}} = \text{Att}(Q_{-1}, K_{\text{evict}}, V_{\text{evict}})$
- 8:  $C_q = Q_{-1}$
- 9: **return** Output,  $KV_{\text{compress}}$ ,  $KV_{\text{evict}}$ ,  $C_{\text{weight}}$ ,  $C_{\text{out}}$ ,  $C_q$

---

**Algorithm 2** CaliDrop Decode

---

**Require:** Current query  $Q_t$ ,  $KV_{\text{compress}}$ ,  $KV_{\text{evict}}$ ,  $C_{\text{weight}}$ ,  $C_{\text{out}}$ ,  $C_q$ , thresholds  $\theta_1 < \theta_2$

- 1: Compute attention: Output,  $A_{\text{weight}} = \text{Att}(Q_t, K_{\text{compress}}, V_{\text{compress}})$
- 2: Compute the similarity of the current query and the historical query:  $\rho \leftarrow \cos(Q_t, C_q)$
- 3: **if**  $\rho < \theta_1$  **then**
- 4:   Reload  $KV_{\text{evict}}$  and perform recomputation:
- 5:    $C_{\text{weight}} = \sum \exp\left(\frac{Q_{-1} * K_{\text{evict}}^T}{d_k}\right)$
- 6:    $C_{\text{out}} = \text{Att}(Q_{-1}, K_{\text{evict}}, V_{\text{evict}})$
- 7:    $C_q = Q_t$
- 8:   Add calibration with Equation 1: Output =  $\alpha_i \cdot \text{Output} + \alpha_j \cdot C_{\text{out}}$
- 9:   **return** Output
- 10: **else if**  $\rho > \theta_2$  **then**
- 11:   Add calibration with Equation 1: Output =  $\alpha_i \cdot \text{Output} + \alpha_j \cdot C_{\text{out}}$
- 12:   **return** Output
- 13: **else**
- 14:   **return** Output
- 15: **end if**

---

whether recomputation should be performed and calibration should be applied. We calculate the cosine similarity between the current query and the retained historical query. If the cosine similarity is lower than  $\theta_1$ , we consider the current query and historical query to be sufficiently distant. In this case, we reload the evicted KV cache, recompute the attention output with the current query, and update the historical query, the softmax denominator, and the attention output. This hyper-parameter controls the frequency of recomputation, thus controlling the additional computation overhead. If the cosine similarity is higher than  $\theta_2$ , we assume the current query and the historical query are sufficiently similar, and we add calibration because we believe this calibration is likely to improve accuracy. When the cosine similarity lies between the two thresholds, no recomputation or calibration is performed.  $\theta_1$  and  $\theta_2$  work together to balance the accuracy of calibration and the additional computational overhead. The prefilling and decoding procedures of CaliDrop are formally described in Algorithms 1 and 2, respectively.

## 4 Experiments

### 4.1 Experiment Setup

#### 4.1.1 Models and Benchmarks

We test our method on three LLMs: Mistral-7B-Instruct [17], LLaMA-3-8B-Instruct, and LLaMA-3-70B-Instruct [10]. These models are chosen for their strong performance and wide utilization in natural language processing tasks.

To thoroughly evaluate the capabilities of these models with different methods, we use three benchmarks that focus on different aspects of language understanding and reasoning.

Method	Performance Metrics															
	Single-Document QA			Multi-Document QA			Summarization			Few-shot Learning			Synthetic		Code	
	MF-en	Qasper	HotpotQA	2WikiQA	GovReport	MultiNews	TREC	TriviaQA	SAMSum	PCount	PRe	Lcc	RB-P	Avg.		
	18409 3619 9151 4887 8734 2113 5177 8209 6258 11141 9289 1235 4206															
FullKV	48.54	24.35	32.92	21.87	33.05	25.77	67.00	86.84	40.95	5.40	91.00	57.24	49.84	44.98		
	Mistral-7B-Instruct, KV Size = Full															
SLM	22.76	10.31	16.59	14.09	13.41	12.21	35.67	75.93	26.47	3.66	64.60	41.27	35.41	28.64		
+CaliDrop	29.62	13.29	22.54	15.70	20.09	19.14	54.00	78.68	30.71	7.09	63.56	44.62	37.99	<b>33.62</b>		
H2O	32.91	13.15	17.60	14.29	19.56	18.99	39.33	79.77	35.80	5.09	74.76	48.19	40.14	33.81		
+CaliDrop	37.39	17.73	22.19	16.93	23.03	22.01	56.00	83.69	37.12	5.32	77.89	49.31	42.88	<b>37.81</b>		
SnapKV	34.46	12.87	20.11	15.52	17.33	16.37	39.00	81.14	35.14	6.89	73.55	47.05	39.80	33.79		
+CaliDrop	39.16	16.94	22.90	17.67	21.83	21.38	55.33	84.25	37.09	7.17	80.33	46.72	41.93	<b>37.90</b>		
	Mistral-7B-Instruct, KV Size = 64															
SLM	22.66	8.23	18.15	14.98	14.72	14.25	41.00	79.27	34.82	3.74	40.32	48.47	39.08	29.21		
+CaliDrop	30.34	12.31	22.55	16.61	20.47	20.39	53.33	79.95	36.03	7.14	54.29	50.62	41.58	<b>34.28</b>		
H2O	32.94	13.75	18.72	15.08	21.20	20.71	43.00	82.20	37.69	6.38	82.50	51.3	42.55	36.00		
+CaliDrop	37.74	18.60	23.47	17.62	23.78	22.37	55.67	85.54	38.88	5.95	83.92	51.50	44.86	<b>39.22</b>		
SnapKV	37.44	14.85	21.45	15.48	20.76	20.15	47.33	84.46	37.34	5.56	85.22	51.04	42.50	37.20		
+CaliDrop	41.83	18.75	24.52	18.12	23.68	22.23	56.33	86.19	37.90	5.63	86.14	51.68	44.53	<b>39.81</b>		
	Mistral-7B-Instruct, KV Size = 128															
FullKV	40.56	37.54	49.81	34.93	31.04	25.58	69.67	89.85	40.50	12.94	83.67	56.58	51.01	47.98		
	LLaMA-3-8B-Instruct, KV Size = Full															
SLM	24.73	20.83	43.86	29.93	14.59	13.50	36.67	71.49	25.80	14.67	81.00	49.67	42.81	36.12		
+CaliDrop	31.52	27.21	46.79	32.17	17.27	17.27	60.00	81.60	29.45	12.33	78.00	49.39	43.79	<b>40.52</b>		
H2O	31.14	24.28	47.41	31.25	19.02	18.95	38.33	86.77	35.58	8.69	82.33	57.38	48.44	40.74		
+CaliDrop	35.92	28.80	49.58	32.83	20.85	20.86	62.00	88.08	36.95	11.44	82.67	55.75	47.92	<b>44.13</b>		
SnapKV	33.33	25.05	47.56	31.83	16.79	17.20	40.67	86.06	33.81	12.22	77.67	56.27	48.07	40.50		
+CaliDrop	36.91	31.27	49.33	33.97	19.16	19.73	62.33	88.10	35.56	11.55	78.67	54.85	45.55	<b>43.61</b>		
	LLaMA-3-8B-Instruct, KV Size = 128															
SLM	26.21	21.09	43.69	29.56	15.82	16.21	41.33	74.01	33.13	12.67	77.33	56.66	48.40	38.16		
+CaliDrop	30.89	26.28	47.56	31.20	17.98	19.41	61.33	84.39	34.90	12.33	77.67	56.75	46.49	<b>42.09</b>		
H2O	36.17	25.48	48.65	31.74	20.76	20.67	40.00	87.30	36.04	12.33	84.00	58.60	51.23	42.54		
+CaliDrop	34.90	29.42	49.91	32.62	22.43	21.66	62.00	89.42	37.60	13.17	83.67	56.55	49.46	<b>44.83</b>		
SnapKV	37.76	29.75	49.19	32.13	19.89	20.18	47.33	87.86	35.33	11.11	82.33	60.29	50.87	43.39		
+CaliDrop	37.23	30.87	50.45	33.19	21.67	21.57	65.00	89.35	36.94	12.44	83.00	56.19	49.07	<b>45.15</b>		

Table 1: Performance comparison of CaliDrop with SnapKV, H2O, StreamingLLM (SLM) and FullKV on LongBench for LLaMA-3-8B-Instruct and Mistral-7B-Instruct. CaliDrop generally achieves improvements over previous KV cache compression methods across various KV cache sizes and LLMs. The performance strengths of CaliDrop are more evident in small KV cache sizes (i.e. KV Size = 64). Bold text represents the best performance.

**LongBench** [3]: This benchmark is a comprehensive benchmark to evaluate the contextual understanding capabilities of LLMs. It includes tasks such as answering questions, summarizing, and generating code.

**RULER** [16]: RULER is a benchmark to evaluate the long-context modeling capabilities of LLMS. It involves tasks that require understanding and integrating various pieces of information, making it essential for assessing skills in complex multi-hop and aggregation tasks.

**Needle-in-a-Haystack** [23]: This benchmark focuses on testing if models can find important details in long texts. It checks how well models can spot useful information in a lot of text, which is key for tasks like finding facts or answering questions by pulling out parts of the text.

### 4.1.2 Baselines

We evaluate the performance improvement of CaliDrop on top of three baselines.

**StreamingLLM (SLM)** [35] identifies the *attention sink* phenomenon and enables LLMs to process infinitely long texts by maintaining KV cache of the attention sink along with a sliding window of recent tokens.

**Heavy Hitter Oracle (H2O)** [43] measures the importance of tokens using accumulated attention scores. It retains a sliding window along with the KV cache of important tokens, thereby preserving the most useful information.

**SnapKV** [20] achieves KV cache compression by selecting clustered important tokens and utilizing a local window in prefilling phase. It incorporates a clustering algorithm with a pooling layer and captures attention signals from an observation window.

**FullKV** caches all keys and values corresponding to each token, which is the standard approach for KV Cache in transformer-based models.

**Note:** For simplicity, we follow the setting of SnapKV [20] and perform compression only in the prefilling stage. Specifically, during prefilling, token eviction is conducted separately according to the strategies of each baselines. Afterward, the decoding process proceeds with our calibration for better accuracy. Although our approach only focuses on compression during the prefilling stage, it can be easily extended to the decoding stage as well.

#### 4.1.3 Implementation Details

We evaluate the performance of various methods under different compression ratios by retaining  $\{64, 128, 256, 512\}$  tokens of the prompt. For StreamingLLM, we set the number of the attention sinks to 32, and the remaining tokens are allocated as local tokens. For H2O, we evenly split the token budget into important tokens and local tokens, each comprising half of the total. For SnapKV, we set the observation window size to 32 and employ average pooling with a kernel size of 5 for importance evaluation. For CaliDrop, we set  $\theta_1$  to 0.7 and  $\theta_2$  to 0.85, which achieves a trade-off between accuracy improvement and computational efficiency (see Section 5 for more details and exploration experiments). All experiments are conducted on NVIDIA A100 40G GPUs.

### 4.2 Main Results

#### 4.2.1 Results on LongBench

Table 1 and Appendix B show the main results of each method with different models in LongBench. We can conclude from the table that:

**CaliDrop can enhance the performance of various methods:** CaliDrop demonstrates significant performance improvements across a wide variety of tasks, effectively mitigating the performance degradation caused by KV cache compression. Specifically, in the Mistral-7B-Instruct and LLaMA-3-8B-Instruct models with a KV size of 64, CaliDrop consistently outperforms traditional baseline methods such as SLM, H2O, and SnapKV. This suggests that CaliDrop is highly effective in counteracting performance losses, especially under high compression ratios. Moreover, its performance gains are particularly notable in tasks that require multi-hop reasoning and multi-document summarization, highlighting its ability to maintain high performance even in complex and demanding scenarios.

**Marginal benefit of CaliDrop will diminish at higher KV sizes:** As the KV size approaches full capacity, the performance improvement brought by CaliDrop becomes increasingly constrained. This trend can be attributed to the fact that an already large KV cache provides ample information for the model to achieve satisfactory performance. Consequently, the additional benefits derived from calibration are diminished or even reversed. Moreover, as shown in Equation 1, when the KV size increases,  $\alpha_i$  will also increase, while  $\alpha_j$  will decrease, reducing the calibration gain.

#### 4.2.2 Results on RULER

To further test our method in the long context of reasoning ability, we use the advanced long-context benchmark, RULER. In this experiment, we take Mistral-7B-Instruct and LLaMA-3-8B-Instruct as the base model and set the cache size to 64, 128, 256, and 512. As demonstrated in Appendix C, CaliDrop gains a comprehensive performance enhancement across different KV sizes. For example, with a KV size of 64, LLaMA-3-8B-Instruct using SnapKV with CaliDrop reaches **23.32%** compared to the baseline (**14.95%**). As the KV size increases, CaliDrop continues to outperform the baselines. On Ruler, we don't observe the gradual diminishing of the calibration gains as seen in LongBench. This is likely because the KV size of 512 was far from the required capacity for the task. Overall, the results demonstrate the effectiveness of CaliDrop.

#### 4.2.3 Results on Needle-in-a-Haystack

The results in Figure 2 and Appendix D indicate that CaliDrop achieves significant improvements based on token eviction methods across all settings in our experiment. Especially when using LLaMA-3-8B-Instruct with a KV size of 128, CaliDrop increases the accuracy of H2O from 48.5% to 83.8%. With a KV size of 256, when SnapKV is used in combination with CaliDrop, it manages to maintain almost no drop in performance in a context size of 8k. The reason for this enhancement is CaliDrop's ability to calibrate attention outputs using historical data, which helps maintain the integrity of attention mechanisms despite the compression of the KV cache. This calibration process

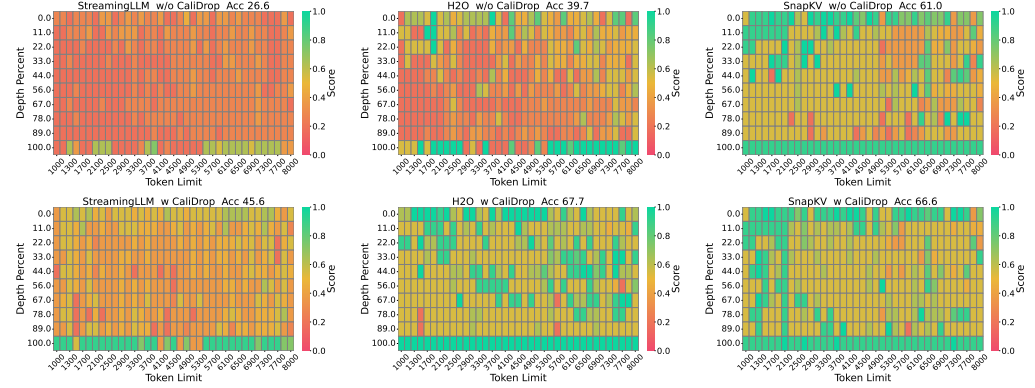


Figure 2: Results of Needle-in-a-Haystack on LLaMA-3-8B-Instruct with 8k context size and 64 KV size. The vertical axis of the figure represents the depth percentage, and the horizontal axis represents the token length.

Group	MF-en	Qasper	HipotQA	2WikiQA	GovReport	MultiNews	TREC	TriviaQA	SAMSum	pCount	Pre	Lcc	RB-P	Avg
R=0.80	L=0.60	36.80	30.28	49.46	32.78	20.70	20.80	61.67	88.62	36.21	13.28	82.00	61.33	51.24
	L=0.65	37.63	31.67	49.73	32.74	21.14	21.19	63.67	88.61	37.13	12.89	83.33	58.09	50.37
	L=0.70	37.99	30.80	49.53	32.66	22.26	21.81	65.33	88.95	37.60	12.11	83.00	58.08	49.67
	L=0.75	38.53	33.60	48.73	32.05	22.79	22.11	65.33	89.01	38.83	10.78	83.00	58.60	49.42
	L=0.80	38.66	32.71	48.85	31.88	23.77	22.79	65.67	88.64	38.29	12.00	82.67	57.39	48.38
R=0.85	L=0.60	37.98	31.74	49.05	32.71	20.50	20.64	59.67	88.77	36.31	12.22	82.33	60.65	51.24
	L=0.65	36.94	31.43	49.64	33.16	20.91	21.08	62.67	88.75	36.38	12.44	83.33	57.81	50.88
	L=0.70	37.23	30.87	50.45	33.19	21.67	21.57	65.00	89.35	36.94	12.44	83.00	56.19	49.07
	L=0.75	37.84	32.47	49.78	34.12	22.61	22.09	64.33	89.25	37.65	11.78	83.33	58.70	51.34
	L=0.80	38.94	33.85	49.74	34.15	24.19	22.80	64.33	89.53	38.74	11.44	84.00	59.11	51.22
R=0.90	L=0.60	37.51	30.88	49.00	33.47	20.49	20.52	55.33	88.54	35.85	13.11	83.00	60.17	52.70
	L=0.65	38.10	31.47	49.12	33.68	20.56	20.82	59.00	87.90	36.04	12.44	82.67	58.73	51.86
	L=0.70	39.06	31.24	50.51	33.45	21.34	21.35	59.67	89.06	36.18	12.22	83.00	58.70	51.79
	L=0.75	37.77	32.84	49.77	33.52	21.89	21.85	58.33	89.65	36.93	13.78	83.33	59.91	52.18
	L=0.80	40.46	33.57	50.17	34.83	23.17	22.06	58.67	90.03	37.75	11.78	83.33	58.90	52.52

Table 2: The influence on accuracy of the left threshold and the right threshold. The experiments are conducted on LongBench with LLaMA-3-8B-Instruct, SnapKV, and a KV size of 128.

ensures that the model can still effectively process long contexts, thereby mitigating the performance degradation caused by token eviction.

## 5 Discussion

CaliDrop has two key hyper-parameters:  $\theta_1$  and  $\theta_2$ .  $\theta_1$  controls the frequency of recomputations, while  $\theta_2$  determines the conditions under which calibration is deemed acceptable.

These hyper-parameters directly influence the model’s throughput and accuracy. Throughput is primarily affected by  $\theta_1$ , as it is directly tied to the frequency of recomputations. Accuracy, however, is influenced by both  $\theta_1$  and  $\theta_2$ .  $\theta_1$  affects calibration quality, with more frequent recomputations leading to better calibration.  $\theta_2$  determines the criteria for when calibration is considered acceptable. If the conditions are too strict, the model may fail to fully leverage the benefits of calibration. On the other hand, if the conditions are too lenient, the model may suffer from low-quality calibration, which could reduce accuracy. Therefore, in this section, we focus on how to improve accuracy while minimizing the decrease in model throughput.

### 5.1 Influence on Accuracy

Table 2 shows the influence on accuracy of  $\theta_1$  and  $\theta_2$ . We can conclude that, with a fixed  $\theta_2$ , higher  $\theta_1$  lead to increased accuracy, which aligns with our hypothesis. This suggests that by increasing the frequency of recomputations, the quality of calibration improves, thereby enhancing accuracy. When  $\theta_1$  is fixed and  $\theta_2$  is varied, accuracy does not follow a consistent trend. This occurs because a high  $\theta_2$  can discard some effective calibration, while a low  $\theta_2$  may introduce potentially harmful calibration. This behavior is also consistent with our hypothesis. Based on these results, we set  $\theta_1 = 0.7$  and  $\theta_2 = 0.85$  for our main experiment.

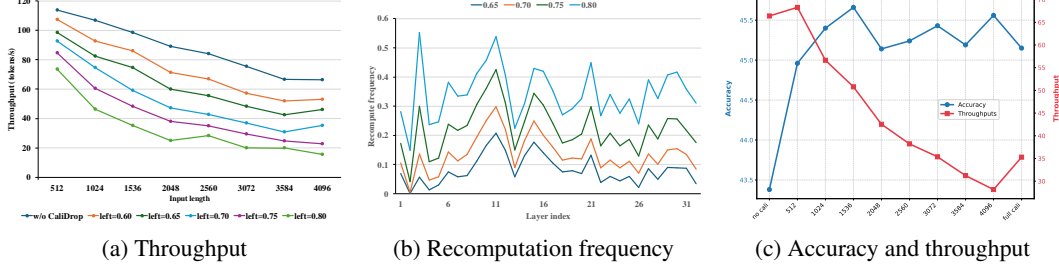


Figure 3: (a) Accuracy and throughput under different calibration sizes. No cali: without calibration. Full cali: all evicted tokens are used for calibration (calibration size =  $\infty$ ). We set  $\theta_1 = 0.7$  in our experiment. (b) Throughput of CaliDrop under different input lengths and  $\theta_1$ . (c) Recomputation frequency of CaliDrop in different layers under different  $\theta_1$ .

## 5.2 Speed Analysis

The speed of CaliDrop is primarily influenced by  $\theta_1$ . To explore this, we conduct experiments using LLaMA-3-8B-Instruct with SnapKV and a KV size of 256. We fix the batch size at 4 and set the output length to 128. In the experiments, we vary the input length and  $\theta_1$  while monitoring throughput. The results are presented in Figure 3a. As anticipated, a higher  $\theta_1$  leads to more frequent recomputations, which reduces throughput. Additionally, as the input length increases, CaliDrop’s throughput slows down due to the greater demand for data transfer and computation.

In addition, we also investigate the frequency of recomputation. We conduct experiments on LongBench using LLaMA-3-8B-Instruct with SnapKV and a KV size of 128. We compare the recompute frequency (the ratio of recomputations to total decoding steps) in different layers under different  $\theta_1$  in Figure 3b. We find that the degree of variation in query similarity between different layers is inconsistent, leading to differences in recompute frequencies across layers. Additionally, as observed earlier, a higher  $\theta_1$  leads to more recomputations. Overall, in our main experiment ( $\theta_1=0.7$ ), recompute occurs approximately every eight steps.

## 5.3 Efficiency Optimization

In the main experiment, we have not applied any efficiency optimizations. There are many ways to improve efficiency. In theory, most of the existing KV optimization methods can be used for the offloaded KV cache, such as quantization, token eviction, etc. Other methods like specialized CUDA kernel, page-level I/O [30], communication overlapping is also useful for CaliDrop. We propose a promising method and demonstrate that its theoretical computation is not high (approximately every 8 steps for recalculation), and does not focus on its actual efficiency. Therefore, more efficiency optimization work will be left to future work. We here propose a simple optimization method that better achieves a balance between efficiency and accuracy. During the compression phase, when evicted tokens are offloaded, we introduce a hyper-parameter called the calibration size, which specifies the maximum number of tokens that can be offloaded. We rank the tokens by importance and offload the most important tokens (up to the calibration size) to optimize the efficiency of calibration computation. Figure 3c shows the accuracy of LLaMA-3-8B-Instruct using SnapKV and CaliDrop on LongBench under different calibration sizes, along with throughput results from the experiment setup in Section 5.2. We find that a small calibration size can lead to significant performance improvements with only a modest sacrifice in throughput.

## 6 Conclusion

In this work, we propose CaliDrop, a strategy that enhances token eviction methods at the cost of additional computations. We leverage the similarity between queries to add precomputed calibration for future queries, and offload the evicted tokens for future recomputation. Calidrop effectively improves accuracy based on token eviction methods, allowing them to perform better in scenarios with lower compression ratios. We also explore a series of efficiency-related issues concerning CaliDrop and propose several potential optimization solutions.

## References

- [1] Josh Achiam, Steven Adler, Sandhini Agarwal, Lama Ahmad, Ilge Akkaya, Florencia Leoni Aleman, Diogo Almeida, Janko Altenschmidt, Sam Altman, Shyamal Anadkat, et al. Gpt-4 technical report. *arXiv preprint arXiv:2303.08774*, 2023.
- [2] Joshua Ainslie, James Lee-Thorp, Michiel de Jong, Yury Zemlyanskiy, Federico Lebron, and Sumit Sanghai. Gqa: Training generalized multi-query transformer models from multi-head checkpoints. In *Proceedings of the 2023 Conference on Empirical Methods in Natural Language Processing*, pages 4895–4901, 2023.
- [3] Yushi Bai, Xin Lv, Jiajie Zhang, Hongchang Lyu, Jiankai Tang, Zhidian Huang, Zhengxiao Du, Xiao Liu, Aohan Zeng, Lei Hou, Yuxiao Dong, Jie Tang, and Juanzi Li. Longbench: A bilingual, multitask benchmark for long context understanding. In Lun-Wei Ku, Andre Martins, and Vivek Srikumar, editors, *Proceedings of the 62nd Annual Meeting of the Association for Computational Linguistics (Volume 1: Long Papers), ACL 2024, Bangkok, Thailand, August 11-16, 2024*, pages 3119–3137. Association for Computational Linguistics, 2024.
- [4] William Brandon, Mayank Mishra, Aniruddha Nrusimha, Rameswar Panda, and Jonathan Ragan Kelly. Reducing transformer key-value cache size with cross-layer attention. *arXiv preprint arXiv:2405.12981*, 2024.
- [5] Zefan Cai, Yichi Zhang, Bofei Gao, Yuliang Liu, Tianyu Liu, Keming Lu, Wayne Xiong, Yue Dong, Baobao Chang, Junjie Hu, et al. Pyramidkv: Dynamic kv cache compression based on pyramidal information funneling. *arXiv preprint arXiv:2406.02069*, 2024.
- [6] Chi-Chih Chang, Wei-Cheng Lin, Chien-Yu Lin, Chong-Yan Chen, Yu-Fang Hu, Pei-Shuo Wang, Ning-Chi Huang, Luis Ceze, Mohamed S Abdelfattah, and Kai-Chiang Wu. Palu: Compressing kv-cache with low-rank projection. *arXiv preprint arXiv:2407.21118*, 2024.
- [7] Guoxuan Chen, Han Shi, Jiawei Li, Yihang Gao, Xiaozhe Ren, Yimeng Chen, Xin Jiang, Zhenguo Li, Weiyang Liu, and Chao Huang. Sepllm: Accelerate large language models by compressing one segment into one separator. *arXiv preprint arXiv:2412.12094*, 2024.
- [8] Alessio Devoto, Yu Zhao, Simone Scardapane, and Pasquale Minervini. A simple and effective  $l_2$  norm-based strategy for kv cache compression. *arXiv preprint arXiv:2406.11430*, 2024.
- [9] Shichen Dong, Wen Cheng, Jiayu Qin, and Wei Wang. Qaq: Quality adaptive quantization for llm kv cache. *arXiv preprint arXiv:2403.04643*, 2024.
- [10] Abhimanyu Dubey, Abhinav Jauhri, Abhinav Pandey, Abhishek Kadian, Ahmad Al-Dahle, Aiesha Letman, Akhil Mathur, Alan Schelten, Amy Yang, Angela Fan, et al. The llama 3 herd of models. *arXiv preprint arXiv:2407.21783*, 2024.
- [11] Yuan Feng, Junlin Lv, Yukun Cao, Xike Xie, and S Kevin Zhou. Ada-kv: Optimizing kv cache eviction by adaptive budget allocation for efficient llm inference. *arXiv preprint arXiv:2407.11550*, 2024.
- [12] Yu Fu, Zefan Cai, Abedelkadir Asi, Wayne Xiong, Yue Dong, and Wen Xiao. Not all heads matter: A head-level kv cache compression method with integrated retrieval and reasoning. *arXiv preprint arXiv:2410.19258*, 2024.
- [13] Suyu Ge, Yunan Zhang, Liyuan Liu, Minjia Zhang, Jiawei Han, and Jianfeng Gao. Model tells you what to discard: Adaptive kv cache compression for llms. *arXiv preprint arXiv:2310.01801*, 2023.
- [14] Yefei He, Luoming Zhang, Weijia Wu, Jing Liu, Hong Zhou, and Bohan Zhuang. Zipcache: Accurate and efficient kv cache quantization with salient token identification. *arXiv preprint arXiv:2405.14256*, 2024.
- [15] Coleman Hooper, Sehoon Kim, Hiva Mohammadzadeh, Michael W. Mahoney, Yakun Sophia Shao, Kurt Keutzer, and Amir Gholami. Kvquant: Towards 10 million context length LLM inference with KV cache quantization. *CoRR*, abs/2401.18079, 2024.
- [16] Cheng-Ping Hsieh, Simeng Sun, Samuel Kriman, Shantanu Acharya, Dima Rekesh, Fei Jia, Yang Zhang, and Boris Ginsburg. Ruler: What’s the real context size of your long-context language models? *arXiv preprint arXiv:2404.06654*, 2024.
- [17] Albert Q. Jiang, Alexandre Sablayrolles, Arthur Mensch, Chris Bamford, Devendra Singh Chaplot, Diego de Las Casas, Florian Bressand, Gianna Lengyel, Guillaume Lample, Lucile Saulnier, Lélio Renard Lavaud, Marie-Anne Lachaux, Pierre Stock, Teven Le Scao, Thibaut Lavril, Thomas Wang, Timothée Lacroix, and William El Sayed. Mistral 7b. *CoRR*, abs/2310.06825, 2023.

[18] Jordan Juravsky, Bradley Brown, Ryan Ehrlich, Daniel Y Fu, Christopher Ré, and Azalia Mirhoseini. Hydragen: High-throughput llm inference with shared prefixes. *arXiv preprint arXiv:2402.05099*, 2024.

[19] Hao Kang, Qingru Zhang, Souvik Kundu, Geonhwa Jeong, Zaoxing Liu, Tushar Krishna, and Tuo Zhao. GEAR: an efficient KV cache compression recipe for near-lossless generative inference of LLM. *CoRR*, abs/2403.05527, 2024.

[20] Yuhong Li, Yingbing Huang, Bowen Yang, Bharat Venkitesh, Acyr Locatelli, Hanchen Ye, Tianle Cai, Patrick Lewis, and Deming Chen. Snapkv: Llm knows what you are looking for before generation. *arXiv preprint arXiv:2404.14469*, 2024.

[21] Aixin Liu, Bei Feng, Bin Wang, Bingxuan Wang, Bo Liu, Chenggang Zhao, Chengqi Dengr, Chong Ruan, Damai Dai, Daya Guo, et al. Deepseek-v2: A strong, economical, and efficient mixture-of-experts language model. *arXiv preprint arXiv:2405.04434*, 2024.

[22] Aixin Liu, Bei Feng, Bing Xue, Bingxuan Wang, Bochao Wu, Chengda Lu, Chenggang Zhao, Chengqi Deng, Chenyu Zhang, Chong Ruan, et al. Deepseek-v3 technical report. *arXiv preprint arXiv:2412.19437*, 2024.

[23] Nelson F Liu, Kevin Lin, John Hewitt, Ashwin Paranjape, Michele Bevilacqua, Fabio Petroni, and Percy Liang. Lost in the middle: How language models use long contexts. *Transactions of the Association for Computational Linguistics*, 12:157–173, 2024.

[24] Zichang Liu, Aditya Desai, Fangshuo Liao, Weitao Wang, Victor Xie, Zhaozhuo Xu, Anastasios Kyrillidis, and Anshumali Shrivastava. Scissorhands: Exploiting the persistence of importance hypothesis for llm kv cache compression at test time. *Advances in Neural Information Processing Systems*, 36, 2024.

[25] Zirui Liu, Jiayi Yuan, Hongye Jin, Shaochen Zhong, Zhaozhuo Xu, Vladimir Braverman, Beidi Chen, and Xia Hu. KIVI: A tuning-free asymmetric 2bit quantization for KV cache. In *Forty-first International Conference on Machine Learning, ICML 2024, Vienna, Austria, July 21-27, 2024*. OpenReview.net, 2024.

[26] Ziran Qin, Yuchen Cao, Mingbao Lin, Wen Hu, Shixuan Fan, Ke Cheng, Weiyao Lin, and Jianguo Li. CAKE: Cascading and adaptive KV cache eviction with layer preferences. In *The Thirteenth International Conference on Learning Representations*, 2025.

[27] Noam Shazeer. Fast transformer decoding: One write-head is all you need. *arXiv preprint arXiv:1911.02150*, 2019.

[28] Ying Sheng, Lianmin Zheng, Binhang Yuan, Zhuohan Li, Max Ryabinin, Beidi Chen, Percy Liang, Christopher Ré, Ion Stoica, and Ce Zhang. Flexgen: High-throughput generative inference of large language models with a single gpu. In *International Conference on Machine Learning*, pages 31094–31116. PMLR, 2023.

[29] Yutao Sun, Li Dong, Yi Zhu, Shaohan Huang, Wenhui Wang, Shuming Ma, Quanlu Zhang, Jianyong Wang, and Furu Wei. You only cache once: Decoder-decoder architectures for language models. *arXiv preprint arXiv:2405.05254*, 2024.

[30] Jiaming Tang, Yilong Zhao, Kan Zhu, Guangxuan Xiao, Baris Kasikci, and Song Han. Quest: Query-aware sparsity for efficient long-context llm inference. In *Forty-first International Conference on Machine Learning*, 2024.

[31] Hugo Touvron, Louis Martin, Kevin Stone, Peter Albert, Amjad Almahairi, Yasmine Babaei, Nikolay Bashlykov, Soumya Batra, Prajjwal Bhargava, Shruti Bhosale, et al. Llama 2: Open foundation and fine-tuned chat models. *arXiv preprint arXiv:2307.09288*, 2023.

[32] Y Wang, D Ma, and D Cai. With greater text comes greater necessity: Inference-time training helps long text generation. *arXiv preprint arXiv:2401.11504*, 2024.

[33] Zheng Wang, Boxiao Jin, Zhongzhi Yu, and Minjia Zhang. Model tells you where to merge: Adaptive kv cache merging for llms on long-context tasks. *arXiv preprint arXiv:2407.08454*, 2024.

[34] Haoyi Wu and Kewei Tu. Layer-condensed kv cache for efficient inference of large language models. *arXiv preprint arXiv:2405.10637*, 2024.

[35] Guangxuan Xiao, Yuandong Tian, Beidi Chen, Song Han, and Mike Lewis. Efficient streaming language models with attention sinks. In *The Twelfth International Conference on Learning Representations, ICLR 2024, Vienna, Austria, May 7-11, 2024*. OpenReview.net, 2024.

- [36] Fangyuan Xu, Tanya Goyal, and Eunsol Choi. Recycled attention: Efficient inference for long-context language models. *arXiv preprint arXiv:2411.05787*, 2024.
- [37] Dongjie Yang, XiaoDong Han, Yan Gao, Yao Hu, Shilin Zhang, and Hai Zhao. Pyramidinfer: Pyramid kv cache compression for high-throughput llm inference. *arXiv preprint arXiv:2405.12532*, 2024.
- [38] June Yong Yang, Byeongwook Kim, Jeongin Bae, Beomseok Kwon, Gunho Park, Eunho Yang, Se Jung Kwon, and Dongsoo Lee. No token left behind: Reliable kv cache compression via importance-aware mixed precision quantization. *arXiv preprint arXiv:2402.18096*, 2024.
- [39] Hao Yu, Zelan Yang, Shen Li, Yong Li, and Jianxin Wu. Effectively compress kv heads for llm. *arXiv preprint arXiv:2406.07056*, 2024.
- [40] Tianyi Zhang, Jonah Yi, Zhaozhuo Xu, and Anshumali Shrivastava. Kv cache is 1 bit per channel: Efficient large language model inference with coupled quantization. *arXiv preprint arXiv:2405.03917*, 2024.
- [41] Yanqi Zhang, Yuwei Hu, Runyuan Zhao, John Lui, and Haibo Chen. Unifying kv cache compression for large language models with leankv. *arXiv preprint arXiv:2412.03131*, 2024.
- [42] Yuxin Zhang, Yuxuan Du, Gen Luo, Yunshan Zhong, Zhenyu Zhang, Shiwei Liu, and Rongrong Ji. Cam: Cache merging for memory-efficient llms inference. In *Forty-first International Conference on Machine Learning*, 2024.
- [43] Zhenyu Zhang, Ying Sheng, Tianyi Zhou, Tianlong Chen, Lianmin Zheng, Ruisi Cai, Zhao Song, Yuandong Tian, Christopher Ré, Clark W. Barrett, Zhangyang Wang, and Beidi Chen. H2O: heavy-hitter oracle for efficient generative inference of large language models. In Alice Oh, Tristan Naumann, Amir Globerson, Kate Saenko, Moritz Hardt, and Sergey Levine, editors, *Advances in Neural Information Processing Systems 36: Annual Conference on Neural Information Processing Systems 2023, NeurIPS 2023, New Orleans, LA, USA, December 10 - 16, 2023*, 2023.
- [44] Xiabin Zhou, Wenbin Wang, Minyan Zeng, Jiaxian Guo, Xuebo Liu, Li Shen, Min Zhang, and Liang Ding. Dynamickv: Task-aware adaptive kv cache compression for long context llms. *arXiv preprint arXiv:2412.14838*, 2024.
- [45] Lei Zhu, Xinjiang Wang, Wayne Zhang, and Rynson WH Lau. Relayattention for efficient large language model serving with long system prompts. *arXiv preprint arXiv:2402.14808*, 2024.

Method	Performance Metrics													
	Single-Document QA		Multi-Document QA		Summarization		Few-shot Learning		Synthetic		Code			
	MF-en	Qasper	HotpotQA	2WikiQA	GovReport	MultiNews	TREC	TriviaQA	SAMSum	PCount	PRE	Lcc	RB-P	Avg.
	18409	3619	9151	4887	8734	2113	5177	8209	6258	11141	9289	1235	4206	
Mistral-7B-Instruct, KV Size = Full														
FullKV	48.54	24.35	32.92	21.87	33.05	25.77	67.00	86.84	40.95	5.40	91.00	57.24	49.84	44.98
Mistral-7B-Instruct, KV Size = 256														
SLM	24.00	9.30	17.54	14.58	17.21	16.87	48.33	79.98	38.11	4.47	42.48	52.50	40.97	31.26
+CaliDrop	29.26	13.04	22.63	16.25	21.91	21.60	54.67	80.06	38.29	6.24	59.63	53.58	43.33	<b>35.42</b>
H2O	34.18	14.97	19.83	15.66	22.54	21.93	48.00	85.54	39.01	5.99	83.40	54.67	45.42	37.78
+CaliDrop	39.53	18.27	24.62	17.54	24.74	23.17	58.33	85.35	39.31	6.06	85.70	53.05	47.17	<b>40.22</b>
SnapKV	42.87	17.33	24.65	16.65	22.78	22.23	58.00	86.77	38.67	6.40	90.57	54.91	45.69	40.58
+CaliDrop	43.97	22.32	26.46	18.66	24.94	23.11	57.33	86.78	39.23	6.00	90.08	54.56	46.97	<b>41.57</b>
Mistral-7B-Instruct, KV Size = 512														
SLM	24.97	10.47	18.02	14.76	21.20	20.03	53.67	82.12	39.07	5.47	42.49	55.37	43.13	33.14
+CaliDrop	31.47	13.97	24.15	16.18	23.99	22.49	55.33	82.70	39.38	6.67	59.86	55.11	45.59	<b>36.68</b>
H2O	36.32	16.50	21.03	16.29	24.19	23.24	53.67	86.58	39.52	6.19	86.37	55.7	47.09	39.44
+CaliDrop	41.43	20.29	26.27	17.73	25.90	24.13	56.67	86.56	39.83	6.63	86.88	55.42	46.83	<b>41.12</b>
SnapKV	45.24	20.09	26.64	18.27	25.18	23.25	62.67	86.51	39.45	5.73	92.22	57.09	47.85	42.32
+CaliDrop	45.03	22.27	29.66	20.73	26.60	23.81	86.86	39.21	5.77	92.33	55.56	47.84	<b>42.67</b>	
LLaMA-3-8B-Instruct, KV Size = Full														
FullKV	40.56	37.54	49.81	34.93	31.04	25.58	69.67	89.85	40.50	12.94	83.67	56.58	51.01	47.98
LLaMA-3-8B-Instruct, KV Size = 256														
SLM	26.78	22.31	42.52	29.17	18.51	19.29	50.67	80.23	36.52	15.00	78.33	58.52	51.56	40.72
+CaliDrop	33.11	25.70	47.92	31.40	20.06	21.31	63.33	84.59	37.44	12.69	78.67	57.55	48.47	<b>43.25</b>
H2O	35.78	28.26	48.71	31.51	21.78	21.44	45.33	89.45	37.92	12.11	83.67	60.02	51.56	43.66
+CaliDrop	36.04	30.67	49.36	33.27	23.03	22.60	63.00	90.06	38.69	12.94	83.67	58.03	52.24	<b>45.66</b>
SnapKV	38.45	30.77	49.70	33.80	22.15	21.71	57.00	89.28	36.79	12.11	84.00	60.22	53.11	45.31
+CaliDrop	39.11	32.72	50.08	33.63	23.49	22.54	66.00	89.99	38.04	13.33	83.67	56.57	51.36	<b>46.19</b>
LLaMA-3-8B-Instruct, KV Size = 512														
FullKV	47.44	44.15	62.12	54.97	31.52	25.21	71.33	91.24	43.56	22.33	89.33	61.71	63.30	54.48
LLaMA-3-70B-Instruct, KV Size = Full														
SLM	30.69	24.51	53.82	50.26	15.28	14.58	38.00	86.66	28.53	22.67	89.00	53.77	46.60	42.64
+CaliDrop	39.31	31.52	54.58	50.95	17.85	18.45	59.67	85.03	30.83	22.67	89.00	50.82	50.45	<b>46.24</b>
H2O	42.98	30.01	58.08	52.90	20.45	20.87	42.00	89.74	38.49	22.44	88.67	56.72	54.55	47.53
+CaliDrop	44.06	35.00	58.12	52.11	21.51	21.53	62.00	90.55	39.65	22.44	88.67	58.37	55.91	<b>49.99</b>
SnapKV	42.35	31.78	58.51	53.62	18.44	19.15	44.00	89.41	37.12	22.67	88.33	57.42	54.10	47.45
+CaliDrop	43.23	34.60	58.22	51.73	20.03	20.52	64.00	91.18	38.91	23.00	88.67	56.90	54.59	<b>49.66</b>

Table 3: Performance comparison of CaliDrop with SnapKV, H2O, StreamingLLM (SLM) and FullKV on Long- Bench for LLaMA-3-8B-Instruct, Mistral-7B-Instruct and LLaMA-3-70B-Instruct. CaliDrop generally achieves improvements over previous KV cache compression methods across various KV cache sizes and LLMs. Bold text represents the best performance.

## A Limitations

Although CaliDrop can significantly improve the accuracy of existing token eviction methods, it still has some limitations:

- The performance improvement brought by CaliDrop comes at the cost of throughput. It can be seen as an intermediate state between KV cache offloading and KV cache compression. It achieves a balance between accuracy and efficiency through offloading and infrequent recomputations. In Discussion, we analyze its efficiency in detail and explore several optimization directions, but leave more optimization methods for future work.
- When the KV cache budget is very high, the token eviction method may already achieve accuracy close to that of Full KV. In such cases, CaliDrop cannot further improve accuracy because its upper bound is Full KV. Like we have already discussed in the analysis of LongBench, as the KV size increases, the marginal benefits of CaliDrop diminish.
- For simplicity, we only consider the setting of SnapKV, where compression is applied solely during the prefilling phase. Although CaliDrop can be easily extended to the decoding phase, addressing efficiency issues in scenarios like long-generation still requires more refined design of the method.

## B More results on LongBench.

Table 3 shows the additional results of LongBench.

Method	Single NIAH			Multi-key NIAH			MQ-NIAH	MV-NIAH	CWE	FWE	$\sqrt{\Delta}$	Avg.
	S-NIAH-1	S-NIAH-2	S-NIAH-3	MK-NIAH-1	MK-NIAH-2	MK-NIAH-3						
LLaMA-3-8B-Instruct, KV Size = Full												
FullKV	100.00	98.20	97.00	99.20	91.60	95.80	99.75	97.45	97.82	82.27	98.28	96.12
LLaMA-3-8B-Instruct, KV Size = 64												
SLM	0	0	0	0	0	0	0	0.12	28.80	0	2.63	
+CaliDrop	1.60	1.20	0	2.20	0.40	0	2.20	1.80	0.58	31.33	4.00	<b>4.12</b>
H2O	20.40	20.80	0	5.40	0.40	0	0.20	0.15	4.62	0.20	2.96	5.01
+CaliDrop	76.60	40.20	0	17.00	7.80	0	15.30	14.50	12.16	3.60	11.24	<b>18.04</b>
SnapKV	58.40	67.20	0	21.40	13.80	0	0.75	0.35	0.16	0.20	2.24	14.95
+CaliDrop	77.60	68.20	0	40.20	32.00	0	12.85	12.70	1.18	2.07	9.68	<b>23.32</b>
LLaMA-3-8B-Instruct, KV Size = 128												
SLM	0.40	1.20	2.40	3.00	0.40	0	2.45	2.45	6.84	52.20	0.64	6.54
+CaliDrop	2.40	2.80	2.40	3.00	0.60	0	5.00	4.00	13.72	51.27	5.96	<b>8.29</b>
H2O	41.00	43.80	2.40	15.00	2.40	0	2.30	0.30	18.00	15.13	7.96	13.48
+CaliDrop	73.60	61.00	2.40	26.20	15.60	0	30.85	22.60	36.94	23.87	16.80	<b>28.17</b>
SnapKV	98.80	87.00	0	60.80	33.80	0	17.15	7.45	4.60	31.33	13.20	32.19
+CaliDrop	99.00	87.20	0	65.80	45.40	0	49.40	40.50	13.94	39.07	24.28	<b>42.24</b>
LLaMA-3-8B-Instruct, KV Size = 256												
SLM	1.40	1.20	2.40	3.00	1.40	1.20	2.45	2.45	17.42	75.60	3.12	10.15
+CaliDrop	2.80	2.80	2.40	4.40	1.60	1.20	5.40	4.05	25.48	70.53	8.48	<b>11.74</b>
H2O	66.60	56.60	2.40	25.00	15.20	0	8.90	1.30	31.64	49.93	20.68	25.30
+CaliDrop	83.20	68.00	2.40	40.60	20.80	0	42.70	29.80	58.18	55.20	38.76	<b>39.97</b>
SnapKV	100.00	92.60	0	90.20	26.00	0	76.40	36.50	13.40	47.67	91.48	52.20
+CaliDrop	100.00	93.20	0	89.80	36.60	0	87.15	73.90	40.90	57.33	94.08	<b>61.18</b>
LLaMA-3-8B-Instruct, KV Size = 512												
SLM	4.00	6.20	8.00	7.00	5.20	3.80	5.25	6.80	35.66	74.00	7.68	14.87
+CaliDrop	6.20	7.40	8.00	8.60	5.60	3.80	8.20	8.00	41.38	75.67	12.64	<b>16.86</b>
H2O	88.20	65.60	2.40	44.00	25.60	1.40	24.30	3.00	46.08	64.33	69.28	39.47
+CaliDrop	93.80	75.80	2.40	53.80	23.40	1.40	59.45	39.50	75.18	70.07	81.84	<b>52.42</b>
SnapKV	100.00	93.60	1.60	96.80	31.00	0.20	91.10	71.65	30.50	56.20	94.36	60.64
+CaliDrop	100.00	94.20	1.40	97.20	37.40	0.20	95.55	86.50	67.24	67.47	96.40	<b>67.60</b>
Mistral-7B-Instruct, KV Size = Full												
FullKV	100.00	100.00	96.40	94.60	99.00	80.60	95.75	92.85	83.72	83.93	96.48	93.03
Mistral-7B-Instruct, KV Size = 64												
SLM	0	0	0	0	0	0	0	0	0.28	6.13	0	0.58
+CaliDrop	0.20	0	0	0	0	0	0	0	1.14	8.20	2.32	<b>1.08</b>
H2O	0	0	0	0	0	0	0	0	3.50	0.07	5.00	0.78
+CaliDrop	6.60	1.80	0	0.20	0.20	0	0.10	0.15	12.30	2.27	12.92	<b>3.32</b>
SnapKV	0.20	0.40	0	0.20	0	0	0	0	0.80	0.07	3.20	0.44
+CaliDrop	9.20	4.40	0	2.60	1.40	0	0.10	0.15	6.38	1.20	8.60	<b>3.09</b>
Mistral-7B-Instruct, KV Size = 128												
SLM	0.40	1.20	2.20	3.00	0.40	0	2.40	2.25	4.26	11.47	0.56	2.56
+CaliDrop	0.40	1.20	2.20	3.00	0.40	0	2.15	2.00	26.96	12.93	2.96	<b>4.93</b>
H2O	2.20	2.20	0.20	3.20	0.20	0	0	0.30	14.40	13.47	11.40	4.32
+CaliDrop	13.20	6.40	0.80	4.40	0.60	0	0.05	1.30	23.10	12.47	25.16	<b>7.95</b>
SnapKV	64.20	23.00	0	8.80	4.00	0	0.05	0.05	2.68	41.20	16.36	14.58
+CaliDrop	79.40	40.00	0	17.60	8.20	0	0.60	3.15	8.26	43.47	27.72	<b>20.76</b>
Mistral-7B-Instruct, KV Size = 256												
SLM	1.40	1.20	2.20	3.00	1.00	0.60	2.35	2.30	9.56	29.93	2.40	5.09
+CaliDrop	1.40	1.20	2.20	3.00	1.00	0.60	2.25	1.85	34.82	32.27	4.60	<b>7.74</b>
H2O	29.40	5.80	2.00	4.20	0.40	0	1.45	0.50	30.00	46.87	22.72	13.03
+CaliDrop	44.80	16.80	2.20	7.80	1.00	0	1.85	1.80	38.90	36.07	42.12	<b>17.58</b>
SnapKV	93.60	54.40	0	35.60	8.60	0	1.55	0.65	8.54	62.60	80.64	31.47
+CaliDrop	95.20	59.80	0.20	43.60	16.20	0	8.50	8.00	23.22	70.27	84.24	<b>37.20</b>
Mistral-7B-Instruct, KV Size = 512												
SLM	3.80	5.60	5.60	5.40	4.00	3.00	5.05	4.40	18.94	58.80	7.04	11.06
+CaliDrop	3.80	5.60	5.60	5.40	4.00	3.00	5.00	4.00	39.12	53.93	8.28	<b>12.52</b>
H2O	74.80	21.00	2.00	9.60	2.20	0.60	1.75	0.50	37.66	65.87	49.24	24.11
+CaliDrop	80.40	33.00	1.80	16.60	4.40	0.60	3.80	1.80	49.04	64.20	67.00	<b>29.33</b>
SnapKV	98.00	75.80	0.60	57.40	20.8	0	10.45	3.60	17.36	71.33	92.68	40.73
+CaliDrop	98.00	77.20	2.80	60.40	28.40	0.60	28.50	13.20	40.78	78.67	92.60	<b>47.38</b>

Table 4: Performance comparison of CaliDrop with SnapKV, H2O, StreamingLLM (SLM) and FullKV on RULER for LLaMA-3-8B-Instruct. Bold text represents the best performance.

## C More results on Ruler

Table 4 shows the results of Ruler.

## D More results on Needle-in-a-Haystack.

Figure 4, 5, 6, 7, 8, 9, 10, 11 show the full results of Needle-in-a-Haystack.



Figure 4: Results of Needle-in-a-Haystack on Mistral-7B-Instruct and LLaMA-3-8B-Instruct with 32k and 8k context size and full KV size. The vertical axis of the figure represents the depth percentage, and the horizontal axis represents the token length.

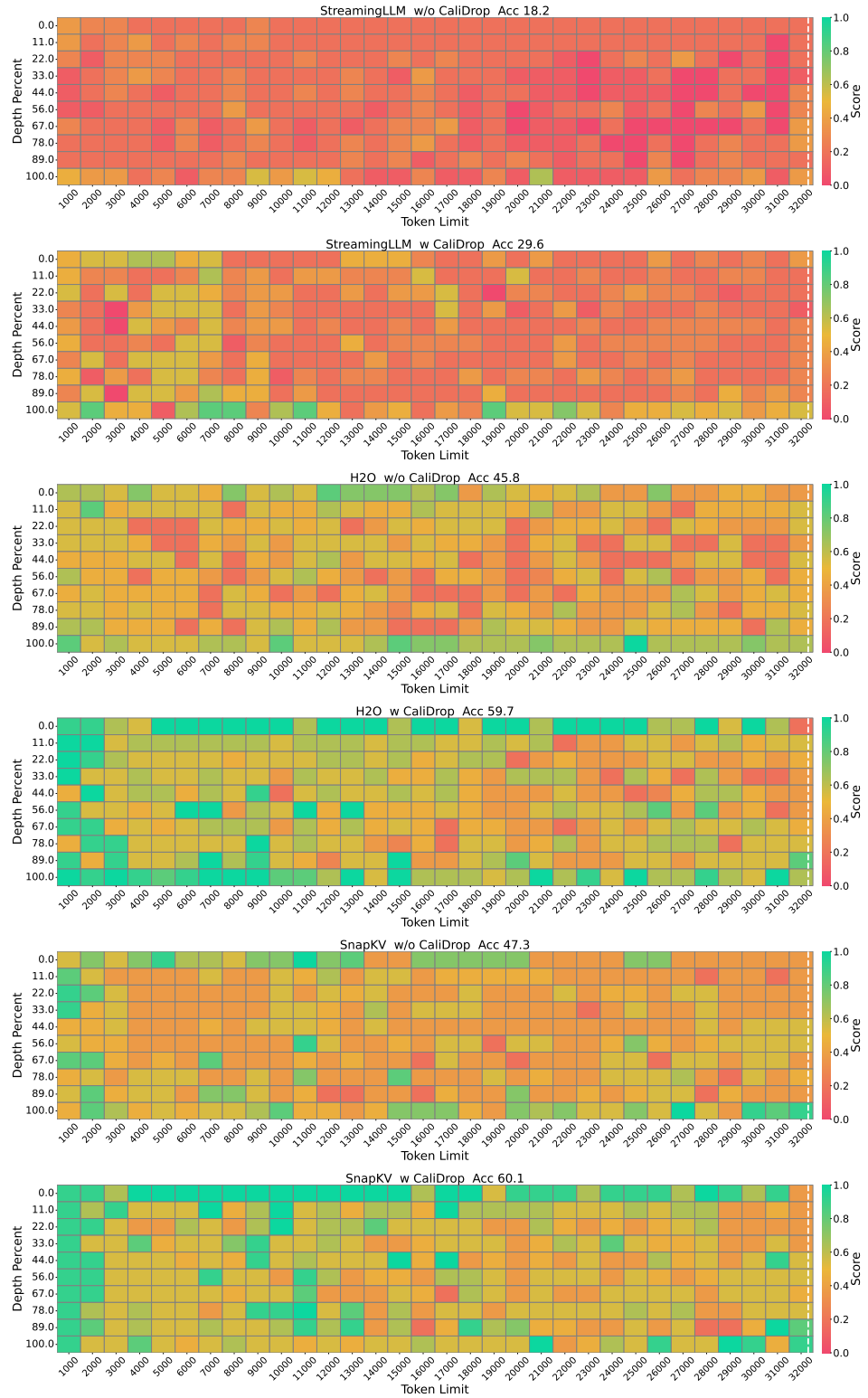


Figure 5: Results of Needle-in-a-Haystack on Mistral-7B-Instruct with 32k context size and 64 KV size. The vertical axis of the figure represents the depth percentage, and the horizontal axis represents the token length.

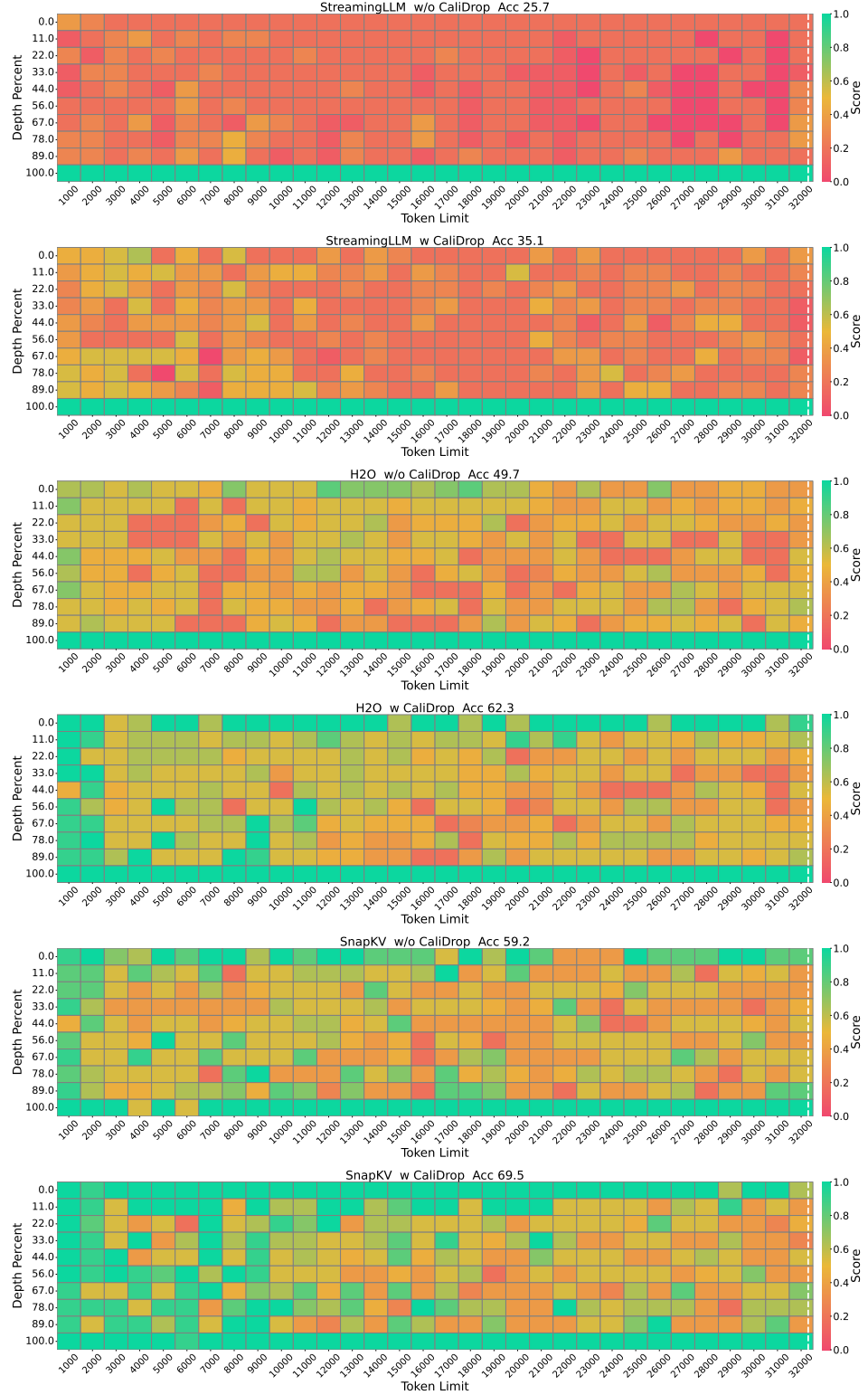


Figure 6: Results of Needle-in-a-Haystack on Mistral-7B-Instruct with 32k context size and 96 KV size. The vertical axis of the figure represents the depth percentage, and the horizontal axis represents the token length.

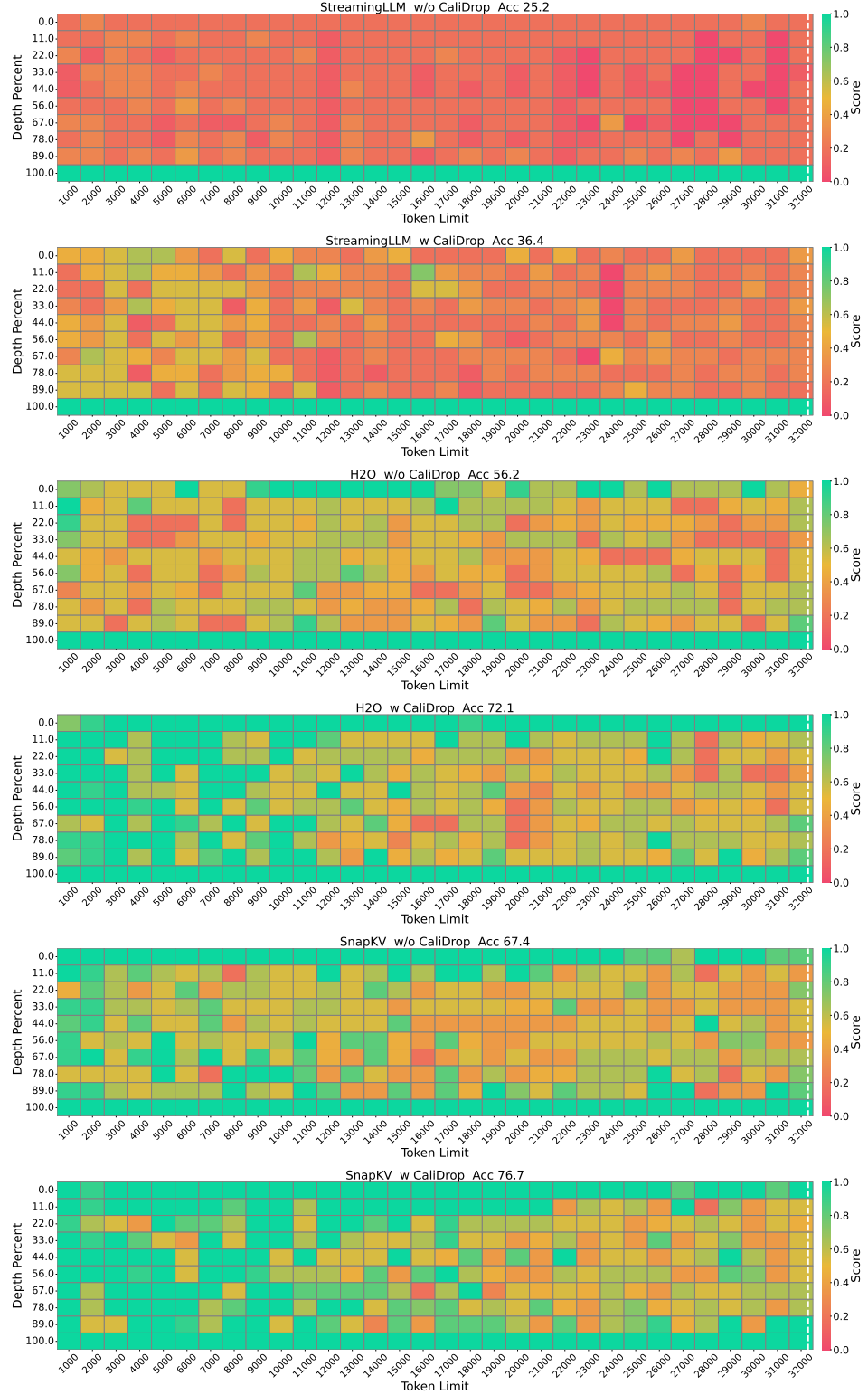


Figure 7: Results of Needle-in-a-Haystack on Mistral-7B-Instruct with 32k context size and 128 KV size. The vertical axis of the figure represents the depth percentage, and the horizontal axis represents the token length.

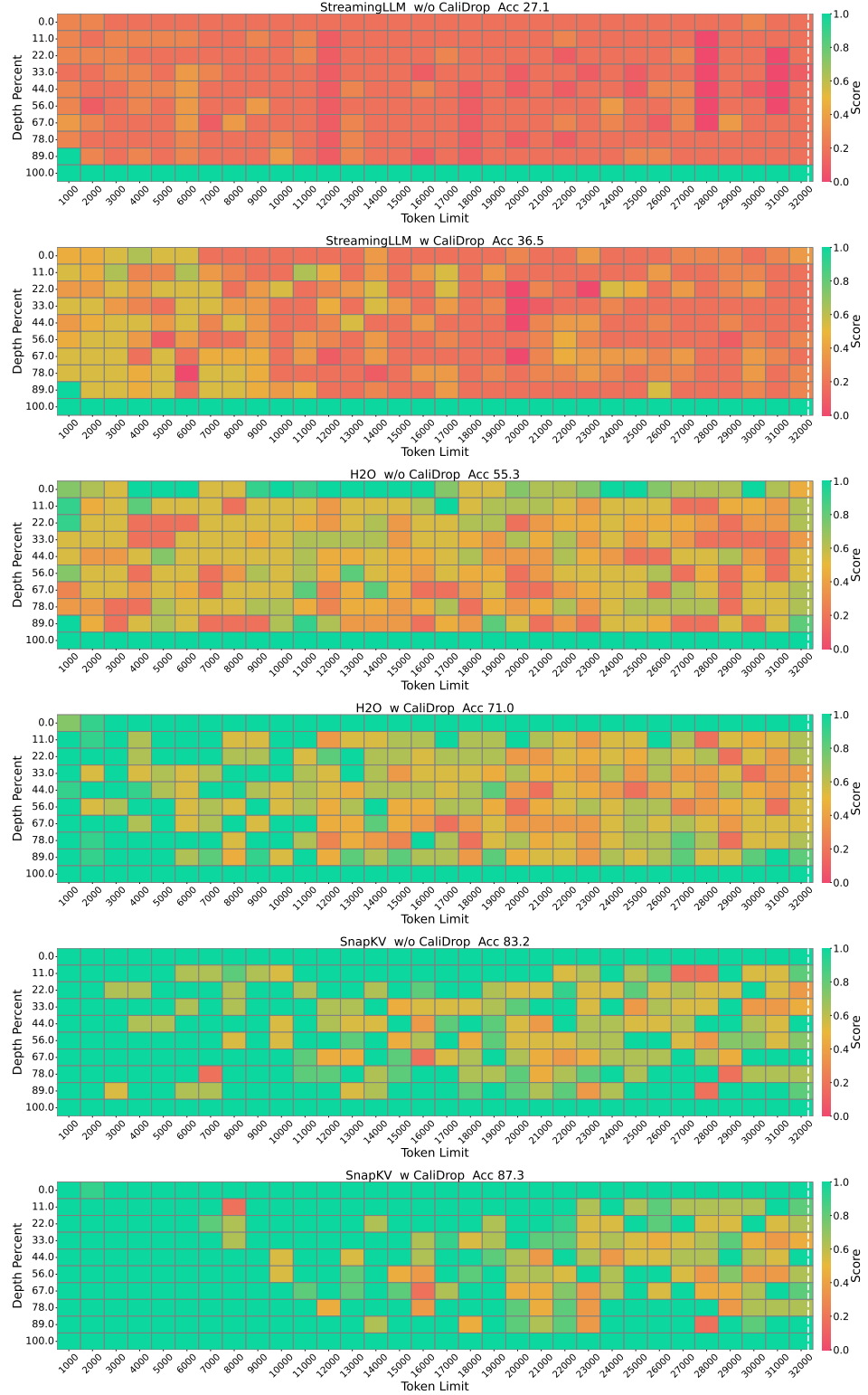


Figure 8: Results of Needle-in-a-Haystack on Mistral-7B-Instruct with 32k context size and 256 KV size. The vertical axis of the figure represents the depth percentage, and the horizontal axis represents the token length.

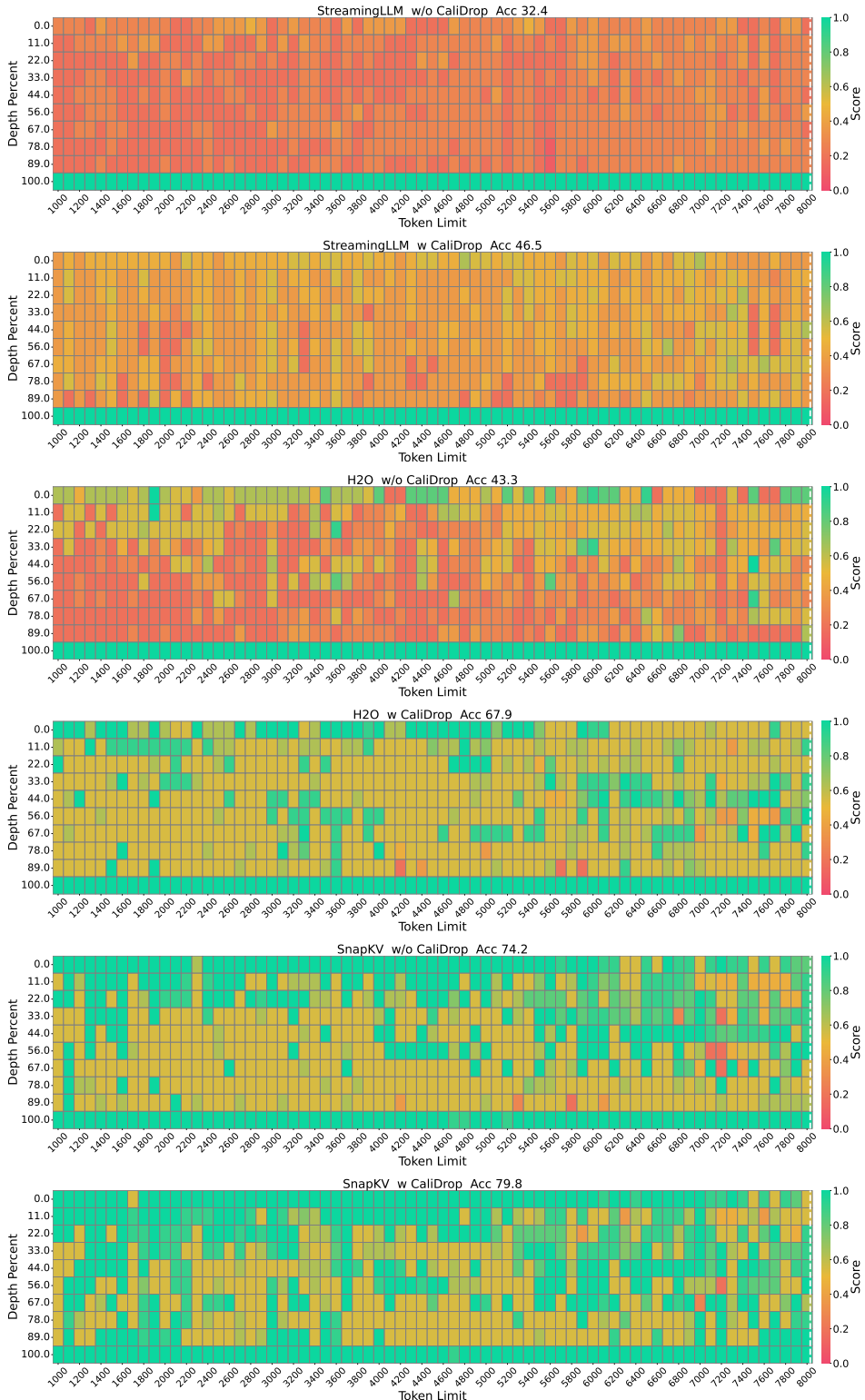


Figure 9: Results of Needle-in-a-Haystack on LLaMA-3-8B-Instruct with 8k context size and 96 KV size. The vertical axis of the figure represents the depth percentage, and the horizontal axis represents the token length.

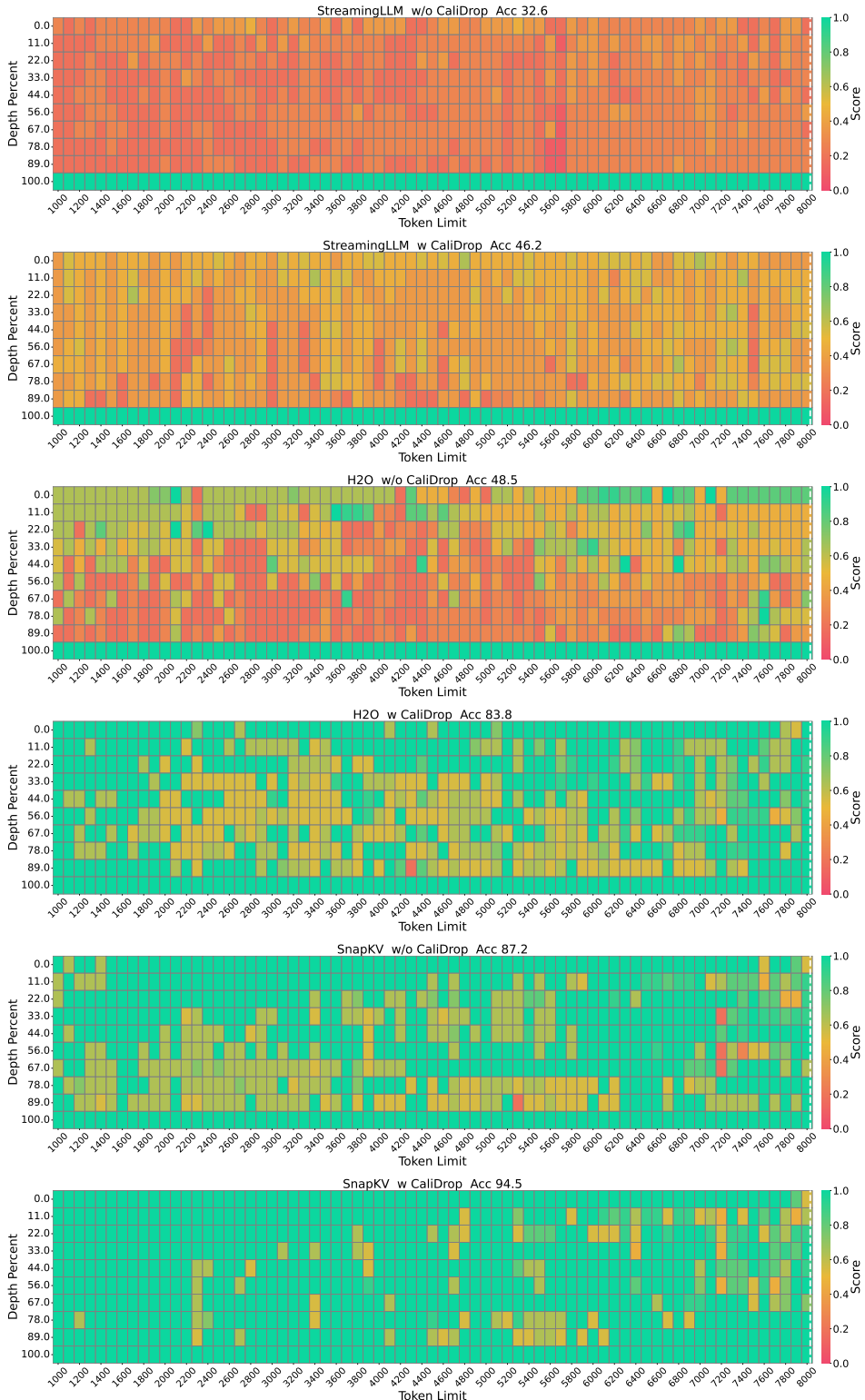


Figure 10: Results of Needle-in-a-Haystack on LLaMA-3-8B-Instruct with 8k context size and 128 KV size. The vertical axis of the figure represents the depth percentage, and the horizontal axis represents the token length.

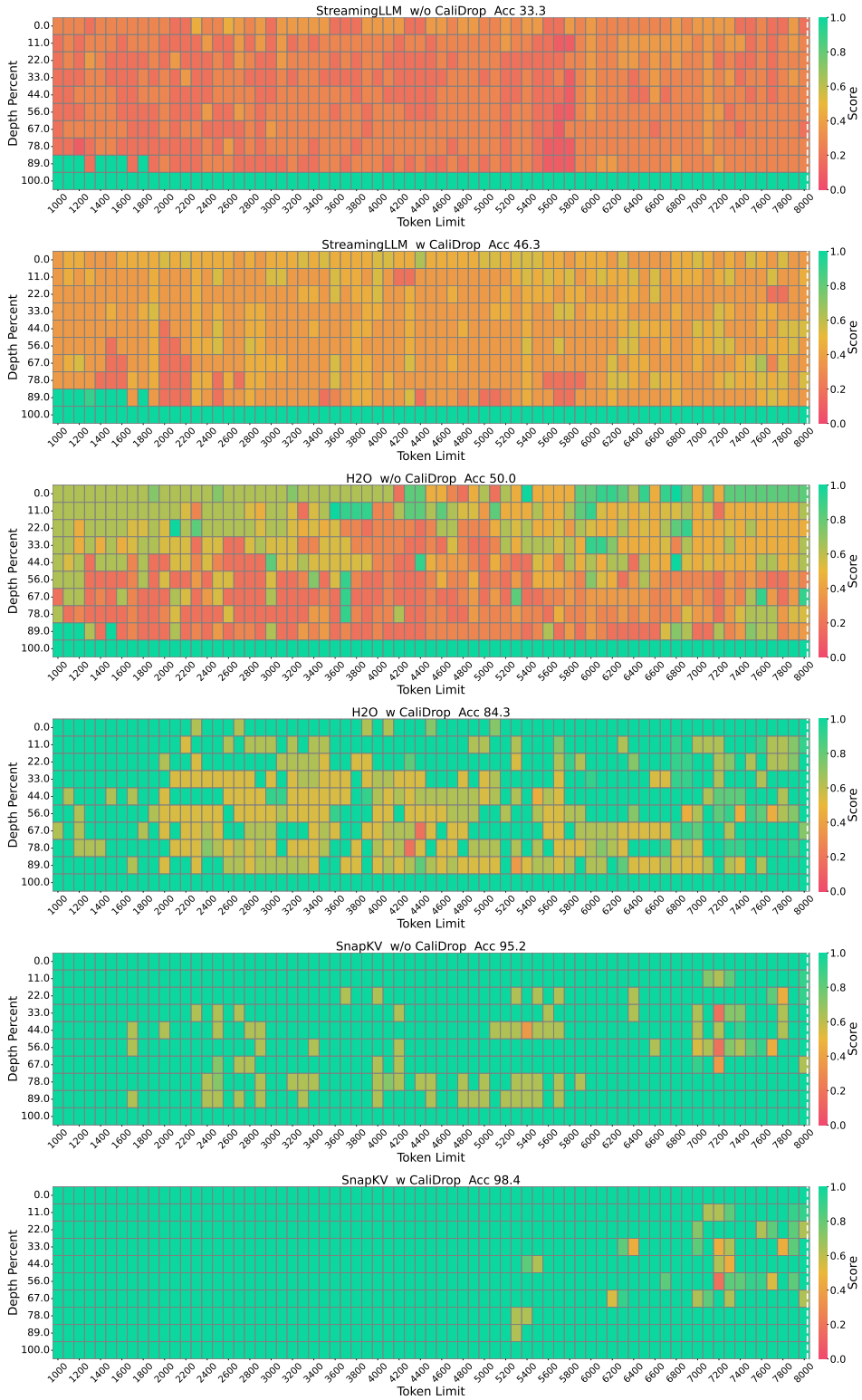


Figure 11: Results of Needle-in-a-Haystack on LLaMA-3-8B-Instruct with 8k context size and 256 KV size. The vertical axis of the figure represents the depth percentage, and the horizontal axis represents the token length.